Optimization of core-valence states of molecules

R. R. Valiev[1,2], J. H. D. Eland[3,4,5], R. Feifel[3,4,a)] and H. Ågren[1]

[1)]*Department of Theoretical Chemistry and Biology, School of Biotechnology, KTH Royal Institute of Technology, SE-106 91 Stockholm, Sweden*

[2)]*Tomsk State University, 36 Lenin Avenue, 634050, Tomsk, Russian Federation*

[3)]*Department of Physics and Astronomy, Uppsala University, Box 516, SE-751 20 Uppsala,Sweden*

[4)]*Department of Physics, University of Gothenburg, Origovägen 6B, SE-412 96 Gothenburg, Sweden*

[5)]*Department of Chemistry, Physical and Theoretical Chemistry Laboratory, Oxford University,South Parks Road, Oxford OX1 3QZ, United Kingdom*

[a)]Electronic mail: raimund.feifel@physics.gu.se

Optimization of core-valence states of molecules

Abstract

Core-valence double electron ionization spectra of a few small molecules - carbon monoxide, ammonia, methyl fluoride and thiophene - are presented and analyzed using the self-consistent field algorithm introduced by Hans Jørgen Jensen 30 years ago. It confirms the utility of this algorithm, frequently employed to obtain stable and sharp convergence of wave functions for the benefit of calculations of a great variety of molecular properties, thus also for optimization of core-valence states and for the interpretation of the corresponding spectra.

Core-valence states, X-ray spectroscopy, double electron ionization spectra, ammonia, thiophene

Subject classification codes: include these here if the journal requires them

1. Introduction

Hans Jørgen Jensens contributions to MCSCF (Multi-Configurational Self-Consistent Field) theory and computation are well known [1–5]. By a four-way development of the theory he could considerably advance the field - by introducing a unitary parameterization of orbtial rotations; by introducing a fully coupled orbital-configurational Hessian in a direct iterative matrix-vector algorithm; by developing a fully second order MCSCF (and SCF) and by implementing the trust radius restricted step method. In addition he developed a number of auxiliary algorithms with relevance for MCSCF optimization. The second order MCSCF method also formed a basis for development of geometric gradients and Hessians for potential energy calculations and transition state searches [6] and for analytic response calculations of general properties [6–8], both by serving as sharply converged reference wave functions but also because the direct MCSCF electronic Hessian matrix - vector operation constitutes a key operation in the calculations of the geometric gradients, Hessians and response functions. Thus the equations to be solved when evaluating molecular properties are similar to those that show up in the MSCCF optimization, in some cases the operations are identical. Access to a stable optimization with minimal residual gradients of the electronic energy thus has had many implications for the use of SCF or MCSCF wave functions. One such application is optimization of core hole states as has been demonstrated in many previous studies using Jensens MCSCF program [4]. The purpose of the present contribution is to highlight the unique possibilities offered by this program for core-hole state optimization and to demonstrate its applicability to a relatively new spectroscopy, namely core-valence double ionization spectroscopy by electron-electron coincidence [9]. We present and discuss results for a few simple molecules.

2. Second order optimization of core hole states

Core hole states, like normal ground states, have traditionally been optimized within the SCF approximation by a series of diagonalizations of the Fock operator, a procedure which is linear with respect to the residual error vector. Bagus was first out, already in 1965[10], to optimize core hole states. He used a maximum overlap criterion,

which can identify the singly occupied core orbital from iteration to iteration. As the core orbital negligibly overlaps with any other orbital that procedure does not collapse variationally. However, for molecules with a high density of orbital eigenvalues straightforward Fock diagonalizations may lead to oscillations and divergence. Various techniques were introduced early on to improve convergence also for core hole states, such as eigenvalue shifts [11], dynamical damping procedures [11], or extrapolation and interpolation of densities [12]. With the introduction of quadratically convergent techniques in SCF calculations, convergence could be guaranteed for the states of lowest energy in a particular symmetry [1,2], which applies to SCF as well as for multiconfiguration SCF. However, a straight application to core hole states is not possible due to the embedding of the core hole states in the electronic continuum. This means that the eigenvalue of the electronic Hessian for the core hole state in question in principle has an infinite root index. A finite basis set makes the root index also finite as the continuum will have a discrete representation but it still remains unknown. Straightforward optimization of such core holes states, even when a single occupancy restriction is imposed, leads to variational collapse. Hans Jørgen Jensen suggested a way out of this problem [3] by applying an intermediate optimization with the core orbital frozen in a restricted active space wave function enforcing the single occupancy restriction. This step brings the wave function to the local quadratically convergent region for a full core hole state optimization involving all orbitals. In this limited variational space the main core hole state or a core hole excited state will have the same root index (order of the Hessian eigenvalue) as an ordinary ground state or lowest excited states of the molecule and the same optimization techniques can be applied with guaranteed and sharp convergence thereby opening applications of, e.g., response techniques for studying X-ray spectroscopies.

Jensen suggested the use of a norm-extended optimization (NEO) algorithm [1,2] for the first intermediate optimization step of core hole states with the core orbital frozen. This choice has several advantages; the core hole state wave function is obtained by solving an eigenvalue equation employing a direct linear transformation with the orbital Hessian. As for normal ground or low-lying states, the structure of the Hessian is monitored and an automatic level shift is computed by means of the trust radius algorithm [1,2]. This means that the number of negative eigenvalues of the projected orbital Hessian is controlled without explicitly determining its eigenvalues. With NEO one automatically finds a level shift so that an optimal step can be taken. The solutions of the eigenvalue equations are given by a series of linear transformations involving the exact orbital Hessian, i.e. quadratically convergent direct SCF. Sharp convergence in the orbital energy gradient is thereby obtained, and a correct variational minimum, i.e. a true local minimum avoiding any saddlepoint that could be encountered in a first-order Fock diagonalization procedure. For core holes states the intermediate frozen core optimization step is thus, as described above, followed by a second optimization where all orbitals are relaxed. In all practical situations the core hole state with core orbital frozen from the first step resides in the local region in the full variational space. The final optimization is then achieved by straight Newton-Raphson minimization towards the stationary point for relaxation of all orbitals including the core orbital. This second optimization step does not require level shifts nor knowledge of the root index, and finds the correct SCF solution including the opened core orbital without variational collapse. We note that this algorithm is implemented and applied to SCF, MCSCF and Kohn-Sham density functional theory in the DALTON program [13].

The algorithm briefly described above has found numerous secure applications among the family of X-ray spectroscopies, like calculations of XPS chemical shifts,

core hole shake-up spectra [14], non-adiabatic couplings [15], X-ray emission and absorption [16]. An early survey is given in Ref. [1]. More recently it has formed the basis for (complex) response theory applications of X-ray spectra, linear [17] as well as non-linear [18], with reference to new X-ray free electron studies. It has also been shown to be a reliable algorithm for optimizing multiple core hole states, such as double core hole states studied in ref. [19] and states with as many as four core holes were optimized in conjunction with a study of hole localization and symmetry breaking in Ref. [20].

3. Experiment

The experiments for the for molecules analyzed in this work were performed at beamlines U49/2-PGM-1 and U49/2-PGM-2 at BESSY-II, Berlin, using a magnetic bottle time-of-flight electron spectrometer designed for coincidence measurements. The spectrometer has a flight tube of about 2.2 m length, and it can detect electrons emitted with kinetic energies from zero to several hundred eVs over essentially the whole solid angle. More detailed descriptions of the multi-electron coincidence technique and the present instrument are given in Refs. [10,22,23]. Because the main decay path of core vacancies of light atoms such as carbon, nitrogen and oxygen is Auger decay, the core-valence double ionisation data were extracted from triple coincidence events, where the first arrival electron is a fast Auger electron, which is expected to be in the range of 220 - 270 eV for the decay of states involving carbon 1s vacancies, 350 - 400 eV for the decay of the states involving the nitrogen 1s hole, and about 510 - 550 eV for the decay of the states involving the oxygen 1s hole. The flight times of the two remaining electrons, with a time reference set by the ionising photon pulse of the ring (e.g. Ref. [22] and refs. therein), are then converted to kinetic energy using the relation

$$E_{kin} = D^2/(t - t_0)^2 + E_0 \quad (1)$$

where t denotes the measured flight time, E_{kin} the electron kinetic energy, and where D (which contains the length of the flight path), t_0 and E_0 are calibration parameters.

The storage ring was operated in single bunch mode, which provides 30 ps light pulses at an inter-pulse spacing of 800.5 ns. Data were recorded at the photon energies of 370 eV for thiophene, 360 eV and 400 eV for CH_3F, 470 eV for NH_3 , and 373 eV and 616 eV for CO, chosen to be well above the thresholds for creation of C-1s, N-1s and O-1s holes, respectively. In order to adjust the electron count rate to a level suitable for coincidence experiments, the exit slit of the monochromator was set to values which correspond to a resolution of about 0.3 eV or better.

The energy resolution of the present magnetic bottle instrument goes from approximately 20 meV at the lowest kinetic energies to a nearly constant numerical resolution of about 50 at high kinetic energies. The time-to-energy conversion was calibrated using Xe 4d photoelectron lines and associated Auger electrons [23] recorded at the photon energy of 105 eV. The sample gases were obtained commercially with a stated purity of >99 %; in the case of thiophene, the vapor pressure of its liquid at room temperature was sufficiently high for achieving a sample gas density in the interaction region of the spectrometer suitable for the experiments without additional heating. In order to remove impurities due to air exposure, when connecting the liquid sample holder to our spectrometer, we used several freeze-pump-thaw cycles. In all cases, the purity of the sample was verified by recording conventional electron spectra both in the valence and core regions in comparison with their spectra known from the literature.

4. Calculations of core valence spectra

A few computational models have earlier been put forward to analyze core-valence spectra [24]. One is based on interaction corrected (Hartree-Fock) orbital energies or the so-called Z+1 approximation (equivalent cores approximation in which the core hole is replaced by a proton), which gives simple orbital interpretations of the spectra and can straightforwardly be used also for larger molecules. Another model was formulated as equivalent to Koopmans' theorem for a two-electron removal, which equates the CV binding energy with two orbital energies instead of one, corrected with a two-electron core-valence repulsion energy and optionally also a core-valence exchange energy which determines the splitting of singlet and triplet states. This gives a qualitative interpretation in terms of a ”shifted single valence electron spectrum”. In fact the valence UV photoelectron spectrum tends to be first choice for analyzing the core valence spectrum of a molecule. However, that strategy can only, at best, give a qualitative interpretation as electrons close together in space experience large electron repulsion (core-valence repulsion values) which implies a significant modification of the sum of single ionization potentials. These can vary between various orbitals, and a large correction to the sum of orbital energies in the modified Koopmans model. It follows that for electrons that are localized in regions that are far apart will have small repulsion energies and pair ionization energies will be close to the sum of the individual ionization potentials. A further limitation is that inflicted by relaxation, namely that core holes generally introduce large relaxation of orbitals and of the two-electron repulsion integrals. For the higher energy part of the CV spectra electron correlation effects become progressively more important, with correlation state satellites, that may be intermixed with the singly ionized states and that are not interpretable by an orbital model. Corrections to the simple models above, with inclusion of electron correlation effects, are called for also for that reason.

The core valence exchange interaction integral, which gives the separation of spin states, obviously also changes with the localization of electrons, in particular the penetration of the valence electron into the core region is of importance for this quantity. The simple Z+1 and modified Koopmans models both neglect this effect, and will thus not produce CV spectra of pure spin states. The assignment of spin states is aggravated by the fact that spin or spin projection is not discriminated in the experiment and it has therefore earlier been assumed (see Niskanen et al, al. [14]) that both spin singlet and triplet states are represented. With all possible spin projections present for the two continuum electrons it was assumed that the residual states appearing in the spectra observed are statistically populated, thus 3/1 for the triplet to singlet ratio. Furthermore, the mechanisms for the double electron ionization is not known, and therefore the transition moments to the continuum and the cross sections are not analyzed. One can though expect that the cross section will vary more strongly with energy close to the double ionization threshold. Owing to these restrictions assignments have been based purely on energetic considerations and this is done also in the present work.

From the outline above it follows that it is preferrable to treat ”spin”, ”relaxation” and ”correlation” in a basic way to analyze core-valence spectra. Jensens spin-adapted, multiconfigurational self-consistent field method [3,25], with the combined norm-extended/second order optimization algorithm guaranteeing convergence without variational collapse, seems therefore to be a preferential choice. Further dynamical correlation can be accounted for by means of perturbation theory (NEVPT2 [26], CASPT2 [27] or RASPT2 [28,29]), see work of Niskanen et al. [30].

However, MCSCF, with our without PT2 correction, is most suitable for the low-lying states, here the core valence onset state, in each spin/spatial symmetry, and for a few states above. For a full spectrum, separate state optimization is not an attractive choice, since the resulting states are overlapping and interacting. Although methodologies are available to correct for that *a posteriori*, the sheer number of states, most of which lack intensity, make a state by state optimization approach unfeasible. A way out was suggested in ref. [24] – to identify the onset by full MCSCF optimization, and to span the spectrum by single and double excitation configuration interaction (SDCI), which catches a great deal of the correlation effect. The orbitals used in the SDCI are optimized for the single core hole state. Thus Jensens algorithm is here used for the onset energies (MCSCF in CASSCF or RASSCF form) for each spatial/spin symmetry and for generating the oribtals of the SDCI. Results of this procedure for carbon monoxide, ammonia, methyl fluoride and thiophene are discussed below.

5. Computational details

The following scheme was applied to all investigated molecules: the energies of lowest singlet and triplet states double ionization core valence (CV) states and the ionization potential of core orbitals were calculated at the RASSCF level of theory. The higher energies of the CV states were calculated using the SDCI method with population of RAS3 by 1 or 2 electrons. Second-order Møller-Plesset perturbation theory has been used as a configuration and orbital generator according to Jensens prescription in Ref. [4]. We assume statistical intensities for triplets versus singlets, thus that the triplet for a given configuration should is 3 times as intensive as the singlet. We have not made a distinction for the intensities in the figures between states with leading core hole single valence hole occupation versus those with leading core hole multiple valence excitations, although it is plausible that the former will be stronger, assuming for instance a shake-off mechanism. All calculations were carried out using the Dalton software [13]. Computational details for each molecule are given below.

5.1. Carbon monoxide

The 1s-AO of carbon was inactive in the calculation of CV-states energies with core hole in 1s of oxygen and 1s-AO of O was included in RAS1 with the occupation by 1 electron. The 1s-AO of oxygen was inactive and 1s-AO of carbon resides in RAS1 with occupation of 1 electron when energies of CV-states with core hole in 1s-AO of carbon were calculated. 9 molecular orbitals (MO) with 11 electrons were included in RAS2 at the RASSCF level of theory and 6 MOs with 11 electrons were included in RAS2 at the SDCI level of theory. 13 MOs were included in RAS3. The aug-cc-pvQZ basis set was used [31].

5.2. Ammonia

RAS1 contained the 1s-AO of nitrogen with occupation of 1 electron. RAS2 included 7 electrons in 8 MOs using the RASSCF method and 3 MOs with the same number of electrons in the SDCI scheme. 14 MOs were included in RAS3 in SDCI. The aug-cc-pvTZ basis set was used [31].

5.3. Fluoromethane

The 1s-AO of fluorine was inactive and RAS1 contained the 1s-AOs of carbon in all calculations. RAS2 included 13 electrons in the 11 MOs at the RASSCF level of

theory and 6 MOs with the same number of electrons in the SD-CI calculations. The RAS3 included 4 MOs. The aug-cc-pvDZ basis set was used [31].

5.4. Thiophene

The one 1s-AO of carbon atom was included in RAS1 with one core hole. The RAS2 included $11a_1$,$3b_1$ and $1a_2$ and the next six MOs in the RASSCF method and only $11a_1$,$3b_1$ and $1a_2$ in the SDCI method. The next six MOs were included in RAS3. The other occupied MOs were inactive. The aug-cc-pvDZ basis set was used.

6. Results and discussion

6.1. Carbon monoxide

The electronic configuration of carbon monoxide with zero charge is $1\sigma^2 2\sigma^2 3\sigma^2 4\sigma^2 1\pi^4 5\sigma^2$. The experimental CV spectrum is presented in Fig. 1. The theoretical energies of CV states, calculated with one core hole in 1s-AO of carbon and 1s-AO of oxygen are combined in Table 1 and illustrated by sticks in Fig. 1. As seen from the figure, the CV spectrum at photon energy hν=616 eV (energy above the 1s-AO of oxygen) is noticeably broader than at hν=373 eV (energy above the 1s-AO of carbon). This difference can be explained using theoretical results in that the CV states are located in a wider region of the spectrum, from 25 eV to 53 eV in the case of core hole in 1s-AO of oxygen in comparison with the case of core hole in the 1s-AO of carbon. In the latter case, the CV-states are located from 27 eV to 41 eV. The first band is formed by S_1 and T_1 states with a valence hole in 5σ, the second band is formed by S_2, S_3 and T_2,T_3 states with the hole in 1π and 4σ MOs in the case of the core hole being in carbon. The other CV states with the core hole in the 1s AO of carbon are located in the region from 35 eV to 41 eV. The 5σ MO has a vacancy for the S_2, S_5, S_8 and T_3, T_5, T_8, T_9 states in the case of core hole in 1s AO of oxygen. Generally, the main difference between the CV-spectra of oxygen and carbon is that more satellite states, characterized by leading two-valence-hole one-particle configurations, appear in the oxygen case.

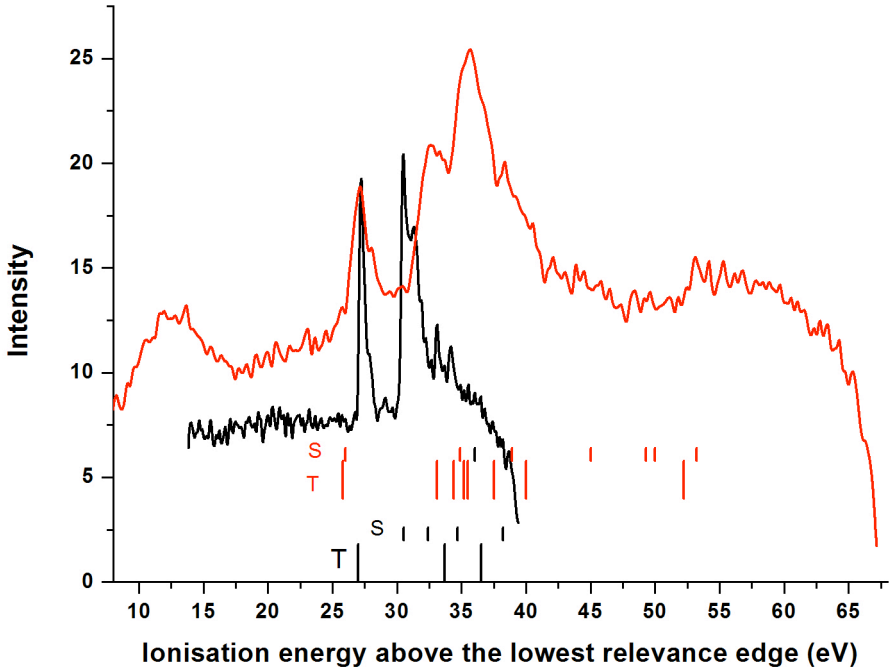

Figure 1. The carbon (black) and oxygen (red) experimental CV spectra of the CO molecule. Computed energies are represented by bars. The relevance edge is K-edge of 1s of O atom for the spectrum with 1s-hole of oxygen and 1s of C atom for the spectrum with 1s-hole of carbon.

6.2. Ammonia

The electronic configuration of the ammonia neutral molecule is $1a_1^2 2a_1^2 1e^4 3\ a_1^2$ in the C_{3V} point group, where $1a_1$ is the core orbital of the nitrogen atom. The experimental CV spectrum of ammonia is shown in Fig. 2. The calculated energies of the CV states are combined in Table 2 and shown as sticks in Fig. 2. As seen, the first band at 24 eV is formed mainly by a triplet state with the valence hole in the $3a_1$ orbital. The band with two peaks between 29 eV and 35 eV is due to singlet and triplets states with hole in the 1e MO, respectively. The third triplet and singlet states form a small intense broad band at 43 eV and 45 eV with a double hole in $3a_1$ and a single occupation in $6a_1$.

Table 1. Calculated energies (in eV) of CV-states for CO molecule

Core hole in Carbon		
State valence hole	Leading configuration	Energy above single core IP
T_1	$5\sigma^1$	27.0
S_1	$5\sigma^1$	30.5
T_2	$1\pi^3$	32.0
S_2	$1\pi^3$	32.4
T_3	$4\sigma^1$	33.7
S_3	$4\sigma^1$	34.7
T_4	$5\sigma^1,1\pi^3,2\pi^{*1}$	36.5
S_4	$5\sigma^1,1\pi^3,2\pi^{*1}$	38.3
Core hole in Oxygen		
State valence hole	Leading configuration	Energy above single core IP
T_1	$5\sigma^1$	25.8
S_1	$5\sigma^1$	26.0
T_2	$1\pi^3$	33.1
T_3	$5\sigma^0,2\pi^{*1}$	34.4
S_2	$5\sigma^0,2\pi^{*1}$	34.9
T_4	$4\sigma^1$	35.2
T_5	$5\sigma^0,6\sigma^{*1}$	35.5
S_3	$1\pi^3$	36.0
T_6	$5\sigma^1,1\pi^2,2\pi^{*2}$	37.5
S_4	$4\sigma^1$	38.9
T_7	$5\sigma^1,1\pi^3,2\pi^{*1}$	40.0
S_5	$5\sigma^1,1\pi^2,2\pi^{*2}$	45.0
S_6	$5\sigma^0,6\sigma^{*1}$	49.3
S_7	$5\sigma^1,1\pi^3,2\pi^{*1}$	50.0
T_8	$5\sigma^0, 6\sigma^1,1\pi^2,2\pi^{*2}$	52.0
S_8	$5\sigma^0,6\sigma^1,1\pi^2,2\pi^{*2}$	53.2

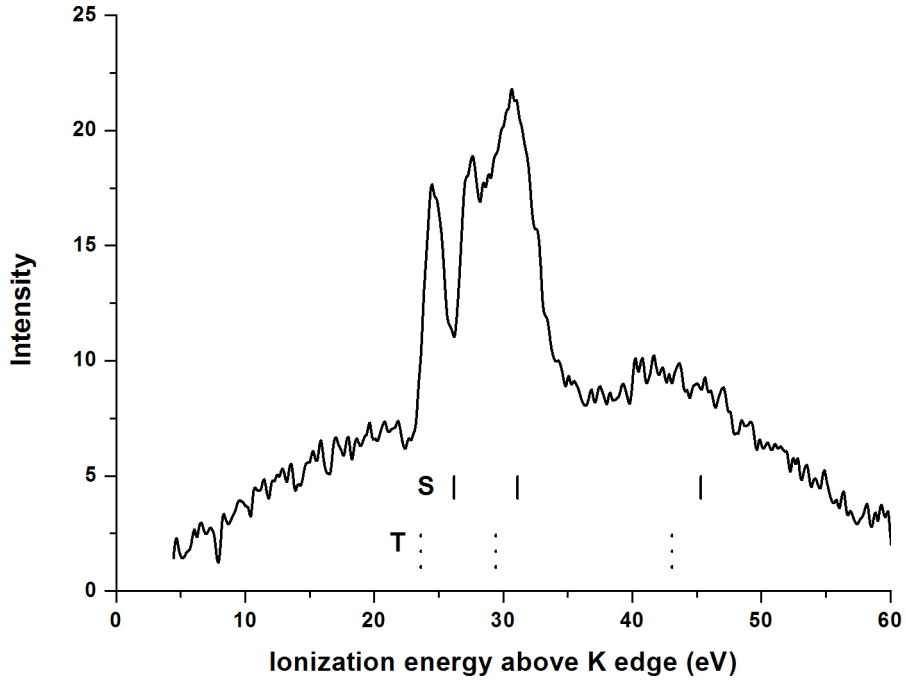

Figure 2. The experimental CV spectrum of NH_3 molecule. Computed energies are represented by bars.

Table 2. Calculated energies (in eV) of CV-states for NH_3 molecule

Core hole in Nitrogen		
State valence hole	Leading configuration	Energy above single core IP
T_1	$3a_1^1$	23.6
S_1	$3a_1^1$	26.2
T_2	$1e^3$	29.4
S_2	$1e^3$	31.1
T_3	$3a_1^0,6a_1^1$	43.1
S_3	$3a_1^0,6a_1^1$	45.3

6.3. Fluoromethane

The electronic configuration of fluoromethane with zero charge is $1a_1^2 2a_1^2 3a_1^2 4a_1^2 1e^4 5a_1^2 2e^4$ in the C_{3V} point group. The experimental CV spectrum (above the K edge of carbon) is shown in Fig. 3 and the calculated energies of the CV-states are given in Table 3. The theoretical results show that the first band is formed by T_1 and S_1 states with a valence hole in 2e. The T_2–T_4, while the S_2–S_4 states with valence occupancy $5a_1^1$, $2e^3 6a_1^{*1}$, $5a_1^0 2e^3 6a_1^{*1}$ form the second band. The third band is

formed by the T_5 and S_5 states with a $1e^3 2e^3 6a_1^{*1}$ configuration. The last band is formed by T_6 and S_6 states with a $5a^1, 2e^3, 6a_1^{*1}$ configuration.

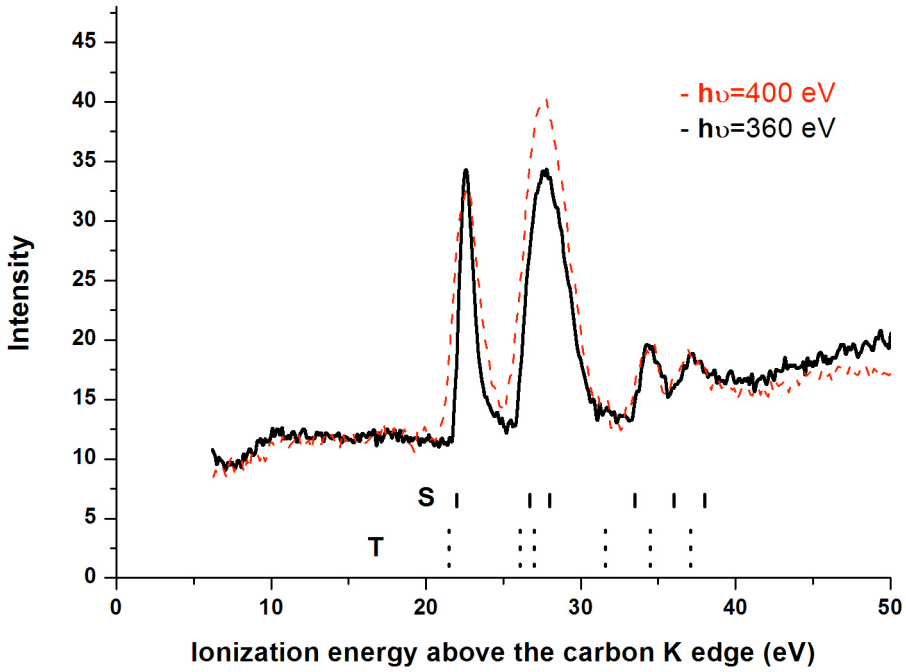

Figure 3. The experimental CV spectrum of CH_3F molecule. Computed energies are represented by bars.

6.4. Thiophene

The electronic configuration of the thiophene neutral molecule is $1a_1^2 1b_2^2 2a_1^2 3a_1^2 2b_2^2 4a_1^2 3b_2^2 5a_1^2 1b_1^2 6a_1^2 4b_2^2 7a_1^2 8a_1^2 5b_2^2 9a_1^2 6b_2^2 10a_1^2 7b_2^2 2b_1^2 11a_1^2 3b_1^2 1a_2^2$ in the C_{2V} point group. The results are presented in Fig. 4 and Table 4. The first band is formed by the S_1–S_3 and T_1–T_3 states. The S_4–S_5 and T_4–T_7 states form the second intense band. The other CV-states produce the third band.

Table 3. Calculated energies (in eV) of CV-states for CH_3F molecule

Core hole in Carbon		
State valence hole	Leading configuration	Energy above single core IP
T_1	$2e^3$	21.5
S_1	$2e^3$	22.0
T_2	$5a_1^1$	26.1
S_2	$5a_1^1$	26.7
T_3	$2e^3, 6a_1^1$	27.0
S_3	$2e^3, 6a_1^{*1}$	28.0

T_4	$5a_1^0,2e^3,6a_1^{*1}$	31.6
S_4	$5a_1^0,2e^3,6a_1^{*1}$	33.5
T_5	$1e^3,2e^3,6a_1^{*1}$	34.5
S_5	$1e^3,2e^3,6a_1^{*1}$	36.0
T_6	$5a^1,2e^3,6a_1^{*1}$	37.1
S_6	$5a^1,2e^3,6a_1^{*1}$	38.0

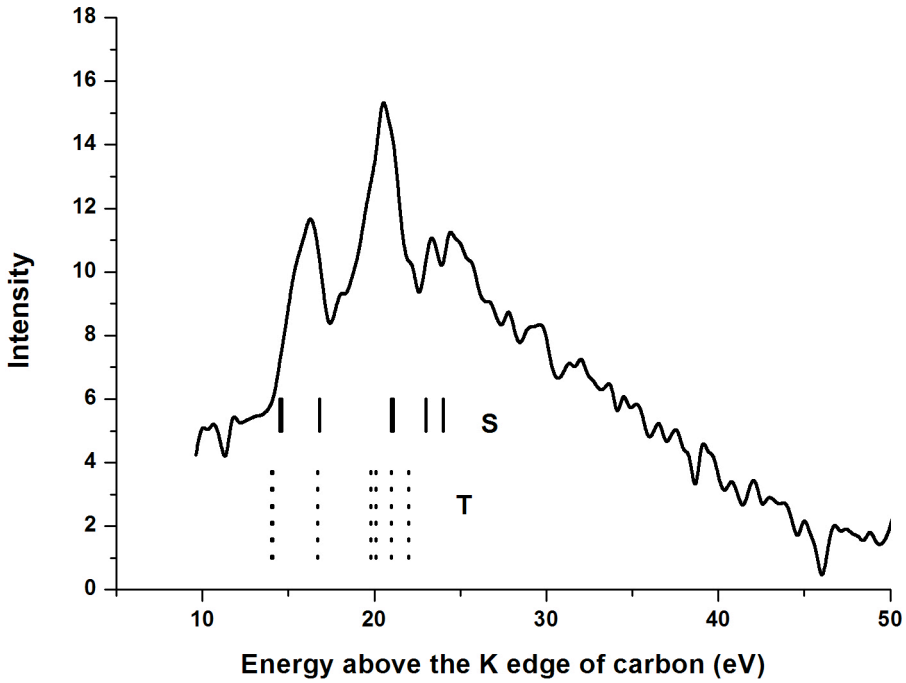

Figure 4. The experimental CV spectrum of thiophene molecule. Computed energies are represented by bars.

7. Discussion

We have demonstrated the utility of the self-consistent field algorithm, introduced by Hans Jørgen Jensen 30 years ago, for calculations of core-valence double electron coincidence spectra. We have presented results for a few small molecules together with their corresponding experimental spectra not published earlier. As for single or multiple core holes states the algorithm gives a stable and sharp convergence of wave functions for the calculations of core-valence onset energies of each spatial and spin core-valence double hole symmetry and for a few states above. It can furthermore favorably be used to generate the orbital basis for dynamical correlation either by configuration interaction or by second order perturbation theory. In this paper we have applied MCSCF orbital based configuration interaction including single and double excitations to span the full measured spectra. Much is known about the accuracy of

core, respectively, valence single electron ionization energies of molecules using quantum chemistry techniques. MCSCF calculations of core-valence spectra will readily catch the extra static correlation which might emerge in the core optimized state electron structure compared to the ground state, and combined MCSCF-PT2 or MCSCF -CI can be expected to possess qualitatively the same inherent accuracy as for the corresponding single electron valence spectrum.

The assignments given are based solely on energetic considerations and can be seen only as tentative because of lack of knowledge of the actual mechanism which generates a cross section for double, core-valence, hole ionization. We can speculate that the core electron shake process is in operation also for core valence ionization, something that also seems supported by the character of leading configurations of some of the higher states computed. In this spirit we can then also assume that the squared coefficient of the leading two-hole core-valence configuration guides the intensity of the particular state in the spectrum. Since spin projection is not discriminated in the experiment, in contrast to normal single core-hole shake-up spectroscopy where only spin doublets are generated, both spin singlet and triplet states are represented and are here assumed to have relative intensities according to their number of spin sublevels. It is nevertheless clear that with two electrons in the continuum generated by direct ionization and with a third electron generated by the Auger process, the calculations of cross sections will face a complicated problem of post-collision "configuration interaction" in the continuum. That is certainly both interesting and challenging.

Table 4. Calculated energies (in eV) of CV-states for the thiophene molecule

Core hole in Carbon		
State valence hole	Leading configuration	Energy above single core IP
T_1	a_2^1	14.0
T_2	$3b_1^1 1a_2^2$	14.1
S_1	a_2^1	14.5
S_2	$3b_1^1 1a_2^2$	14.6
T_3	$11a_1^1$	16.7
S_3	$11a_1^1$	16.8
T_4	$1a_2^0 12a_1^{*1}$	19.8
T_5	$1a_2^0 13a_1^{*1}$	20.1
S_4	$1a_2^0 12a_1^{*1}$	21.0
T_6	$1a_2^0 14a_1^{*1}$	21.0
S_5	$1a_2^0 13a_1^{*1}$	21.1
T_7	$1a_2^0 7b_2^{*1}$	22.5
S_6	$1a_2^0 14a_1^{*1}$	23.0
S_7	$1a_2^0 7b_2^{*1}$	24.5

Acknowledgements

RV and HA acknowledge The Knut and Alice Wallenberg foundation for financial support (GrantNo. KAW-2013.0020). The work has been financially supported by the Swedish Research Council (VR) and the Knut and Alice Wallenberg Foundation, Sweden. We thank the Helmholtz Zentrum Berlin for the allocation of synchrotron radiation beam time. The research leading to these results has received funding from the European Community's Seventh Framework Programme (FP7/2007-2013) under grant agreement no. 312284.

References

[1] H. J.Aa. Jensen and P. Jørgensen, Chem. Phys. 80, 1204 (1984).

[2] H. J.Aa. Jensen and H. Ågren, Chem. Phys. 104, 229 (1986).

[3] H. J.Aa. Jensen, P. Jørgensen, and H. Ågren, J. Chem. Phys. 87, 451 (1987).

[4] H.J. Aa. Jensen, P. Jørgensen, H. Ågren, and J. Olsen, J. Chem. Phys. 88, 3834 (1988).

[5] J. Olsen, B. O. Roos, P. Jørgensen, and H.J.Aa. Jensen, J. Chem. Phys. 89, 2185 (1988).

[6] T. U. Helgaker, J. Almlöf, H.J.Aa. Jensen, and P. Jørgensen, J. Chem. Phys. 84, 6266 (1986).

[7] J. Olsen and P. Jørgensen, J. Chem. Phys. 82, 3235 (1985).

[8] P. Jørgensen, H.J.Aa. Jensen, and J. Olsen, J. Chem. Phys. 89, 3654 (1988).

[9] J. H. D. Eland, O. Vieuxmaire, T. Kinugawa, P. Lablanquie, R. I. Hall, and F. Penent, Phys. Rev. Lett 90, 053003 (2003).

[10] P. S. Bagus, Phys. Rev. 139, A619 (1965).

[11] M. C. Zerner and M. Hehenberger, Chem. Phys. Lett. 62, 550 (1979).

[12] J. Almlöf, P. S. Bagus, B. Liu, D. MacLean, U. I. Wahlgren, and M. Yoshimine, MOLECULE ALCHEMY program package, IBM Research Laboratory (IBM Research Laboratory, 1972).

[13] K. Aidas, C. Angeli, K. L. Bak, V. Bakken, R. Bast, L. Boman, O. Christiansen, R. Cimiraglia, S. Coriani, P. Dahle, E. K. Dalskov, U. Ekström, T. Enevoldsen, J. J. Eriksen, P. Ettenhuber, B. Fernandez, L. Ferrighi, H. Fliegl, L. Frediani, K. Hald, A. Halkier, C. Hättig, H. Heiberg, T. Helgaker, A. C. Hennum, H. Hettema, E. Hjertenæs, S. Høst, I.-M. Höyvik, M. F. Iozzi, B. Jansik, H.J.A. Jensen, D. Jonsson, P. Jørgensen, J. Kauczor, S. Kirpekar, T. Kjærgaard, W. Klopper, S. Knecht, R. Kobayashi, H. Koch, J. Kongsted, A. Krapp, K. Kristensen, A. Ligabue, O. B. Lutnæs, J. I. Melo, K. V. Mikkelsen, R. H. Myhre, C. Neiss, C. B. Nielsen, P. Norman, J. Olsen, J. M. H. Olsen, A. Osted, M. J. Packer, F. Pawlowski, T. B. Pedersen, P. F. Provasi, S. Reine, Z. Rinkevicius, T. A. Ruden, K. Ruud, V. Rybkin, P. Salek, C. C. M. Samson, A. S. de Meràs, T. Saue, S. P. A. Sauer, B. Schimmelpfennig, K. Sneskov, A. H. Steindal, K. O. Sylvester-Hvid, P. R. Taylor, A. M. Teale, E. I. Tellgren, D. P. Tew, A. J. Thorvaldsen, L. Thøgersen, O. Vahtras, M. A. Watson, D. J. D. Wilson, M. Ziolkowski, and H. Ågren, Comput. Mol. Sci. 4, 269 (2014).

[14] H. Ågren and H.J.Aa. Jensen, Chem. Phys. Lett. 137, 431 (1987).

[15] H. Ågren, A. Flores-Riveros, and H.J.Aa. Jensen, Phys. Rev. A 34, 4606 (1986).

[16] H. Ågren, A. Flores-Riveros, and H.J.Aa. Jensen, Physica Scripta 40, 745 (1989).

[17] U. Ekström, P. Norman, V. Carravetta, and H. Ågren, Phys. Rev. Letters 97, 143001 (2006).

[18] T. Fahleson, H. Ågren, and P. Norman, J. Phys. Chem. Letters 7, 1991 (2016).

[19] H. Ågren and H.J.Aa. Jensen, Chem. Phys. 172, 45 (1993).

[20] V. Carravetta and H. Ågren, J. Phys. Chem. A 117, 6798 (2013).

[21] J. H. D. Eland and R. Feifel, Chem. Phys. 327, 85 (2006).

[22] E. Andersson, M. Stenrup, J. H. D. Eland, L. Hedin, M. Berglund, L. Karlsson, Å Larson, and H. Ågren, Phys. Rev. A 78, 023409 (2008).

[23] T. X. Carroll, J. D. Bozek, E. Kukk, V. Myrseth, L. J. Saethre, T. D. Thomas, and K. Wiesner, J. Elec. Spec. Rel. Phen. 125, 127 (2002).

[24] S. Zagorodskikh, M. Vapa, O. Vahtras, V. Zhaunerchyk, M. Mucke, J. H. D. Eland, R. J. Squib, P. Linusson, K. J. Jänkälä, H. Ågren, and R. Feifel, Phys. Chem. Chem. Phys. 18, 2535 (2016).

[25] H.J.Aa. Jensen and H. Ågren, Chem. Phys. Lett 110, 1140 (1984).

[26] C. Angeli, R. Cimiraglia, and J. P. Malrieu. Chem. Phys. Lett., 350, 297 (2001).

[27] K. Andersson, P. Å. Malmqvist, and B. O. Roos, J. Chem. Phys., 96, 1218 (1992).

[28] P. Å. Malmqvist, K. Pierloot, A. R. M. Shahi, C. J. Cramer and L. J. Gagliardi, Chem. Phys., 128, 204109., (2008).

[29] G. Karlström, R. Lindh, P.-E. Malmqvist, B. O. Roos, U. Ryde, V. Veryazov, P.-O. Widmark, M. Cossi, B. Schimmelpfennig, P. Neogrady, and L. Seijo, Computational Material Science 28, 222 (2003).

[30] J. Niskanen, V. Carravetta, O. Vahtras, H. Ågren, H. Aksela, E. Andersson, L. Hedin, P. L. J. H. D. Eland, L. Karlsson, J.-E. Rubensson, and R. Feifel, Phys. Rev. A 82, 043436 (2010).

[31] R. A. Kendall, T. H. Dunning Jr., and R. J. Harrison, J. Chem. Phys., 96, 6796 (1992).